BOLETIN DE LA SOCIEDAD ESPAÑOLA DE
Cerámica y Vidrio
A R T I C U L O

Nonstoichiometry and stability in water of undoped $SrCeO_3$

G. C. MATHER, J. R. JURADO
Instituto de Cerámica y Vidrio, CSIC, Cantoblanco, Madrid, Spain

Strontium cerate is the parent phase of an important class of proton-conducting perovskites with various potential technological applications. Phase formation and structure of $SrCeO_3$ with Sr:Ce nonstoichiometry have been investigated for the series, $Sr_{1\pm x}CeO_{3\pm\delta}$ ($0.98 \le x \le 1.04$). Analyses by EPMA (electron probe micro analysis) and X-ray diffraction (XRD) indicate that, for samples sintered at 1350°C, the main phase is Sr-rich for all x. The accommodation of excess SrO in the bulk phase and/or intergranular regions is discussed. The stability of nominally stoichiometric $SrCeO_3$ was examined in an atmosphere of high water vapour partial pressure (pH_2O) for 2 hours, degrading to $Sr(OH)_2.H_2O$ and CeO_2 for $pH_2O \ge 3.6atm$.

Key words: Ceramic proton conductors; nonstoichiometry; perovskites; stability

No estequiometria y estabilidad en agua de $SrCeO_3$ no dopado

La fase $SrCeO_3$ da origen a una importante familia de perovskitas conductoras protónicas con potenciales aplicaciones tecnológicas. En este trabajo se estudia la formación de la fase y la estructura de $SrCeO_3$ con la relación Sr:Ce no estequiométrica para la serie $Sr_{1\pm x}CeO_{3\pm\delta}$ ($0.98 \le x \le 1.04$). Los análisis por microsonda (EPMA) y difracción de rayos X (DRX) indican que en las muestras sinterizadas a 1350°C, la fase principal es rica en estroncio para todo valor de x. Se discute la posible ubicación del exceso de SrO tanto en la región intergranular como en el propio grano. También se examina la estabilidad de la composición con estequiometría nominal $SrCeO_3$ en una atmosfera con una alta presión de vapor de agua (pH_2O), observándose que la degradación a $Sr(OH)_2.H_2O$ y CeO_2 ocurre a $pH_2O \ge 3.6atm$ (expuesto durante 2 horas).

Palabras claves: Cerámicas conductoras protónicas; no estequiometría; perovskitas; estabilidad.

1. INTRODUCTION

Strontium cerate is the parent phase of an important family of perovskites (ABO_3) which conduct protons in the temperature range, 500-800°C, with potential applications as fuel-cell electrolytes, steam electrolysers, hydrogen sensors and ceramic hydrogen-separation membranes [1-7]. In order to achieve significant levels of proton conductivity, tetravalent Ce is partially substituted with a trivalent cation such as Yb^{3+} ("acceptor-doped") to form oxygen vacancies, $V_o^{\bullet\bullet}$, which are then protonated on exposure to water vapour according to:

$$H_2O + O_o^{\times} + V_o^{\bullet\bullet} \rightarrow 2OH_o^{\bullet} \quad (1)$$

Undoped $SrCeO_3$ has not been intensely studied since proton conductivity is expected to be low as a result of the minimal oxygen-defect concentration. However, oxygen deficiency may be created in cation nonstoichiometric samples either through Sr deficiency:

$$Sr_{Sr} + O_o \rightarrow SrO + V_{Sr}^{''} + V_o^{\bullet\bullet} \quad (2)$$

or Sr excess (Ce deficency):

$$Ce_{ce} + 2O_o \rightarrow CeO_2 + V_{Ce}^{''''} + 2V_o^{\bullet\bullet} \quad (3)$$

Other compensation mechanisms may, instead, take place, including accommodation of excess Ce on the A-site or occupation of the B site with excess Sr. The formation of cation or anion interstitials is expected to be less energetically favourable in the close-packed perovskite structure than either vacancy formation or the occupation of the alternative cation site by the excess cation.

In the related perovskite, $BaCeO_3$, the effects of BaO excess and BaO deficiency have been studied by a number of groups. Some discrepancies have arisen as regard to the extent of A-site deficiency, the role of BaO grain-boundary transport and the probable compensation mechanisms for Ba nonstoichiometry. Haile and co-workers [8,9] found that $BaCeO_3$ accommodates a large excess of BaO (4mol. %) but that BaO deficiency is not tolerated. However, Ma *et. al*. [10] report that $BaCeO_3$ may be prepared with Ba deficiencies up to 5*mol.%*. These authors also observed that, under hydrogen, samples with Ba excess show predominantly ionic conduction ($H^+ + O^{2-}$) while Ba deficient samples are electronic conductors; under oxygen, Ba excess samples showed predominantly electronic conduction whereas Ba-deficient samples are principally oxygen-ion conductors with low conductivity.

Proton conduction in these systems has also been attributed to BaO which often resides at the grain boundaries, particularly in samples with nominal Ba excess [11]. However, establishing whether or not the additional Ba is incorporated in the main phase or grain boundaries (or both) requires detailed analysis. The nominal composition and subsequent interpretation of the effects of cation nonstoichiometry may be significantly altered by the presence of grain-boundary BaO, undetectable by routine X-ray analysis, and evaporation of

BaO as a result of prolonged high-temperature sintering. In addition, the two most intense CeO_2 peaks are overlapped by $BaCeO_3$ reflections, thereby complicating the evaluation of phase limits by XRD alone.

The amorphous vestiges of BaO or SrO at the grain boundaries in these cerate perovskite systems considerably affect stability since reaction takes place with CO_2 from the air to form the carbonate, resulting in decomposition of sintered bodies. Guan *et. al*. [4] report that various perovskites within the $SrO\text{-}CeO_2\text{-}Y_2O_3$ system crumbled after exposure to the air for several days, whereas dense $BaCe(Y)O_3$ perovskites did not. An advantage of the introduction of AO deficiency is that small amounts of unreacted AO at the grain boundaries are less likely to be present. A number of studies on perovskites have, therefore, employed A-site cation substoichiometry to improve stability [12-14].

For applications such as potentiometric hydrogen sensors and separation membranes, significant oxygen-ion transport in the cerate perovskites may be disadvantageous. Although the acceptor-doped Sr analogues have lower proton conductivity than the Ba-containing phases, oxygen–ion conductivity is generally much lower, rendering the Sr-based phases of considerable technological interest. In this paper, the stoichiometry of undoped $SrCeO_3$ and the effect of introducing SrO excess and SrO deficiency in $SrCeO_3$ has been examined employing XRD, Rietveld refinement, scanning electron microscopy (SEM) and EPMA. Stability of $SrCeO_3$ in an atmosphere of high water vapour partial pressure has also been determined.

2. EXPERIMENTAL

Samples were prepared by solid-state reaction of $SrCO_3$ (99.9%+) and CeO_2 (99.9%) in appropriate ratios. The reagents were ball-milled for 2 hours in isopropyl alcohol prior to drying and sieving through a 100μm mesh. The reactant mixture was then fired at 1100°C for 4 hours with a heating/cooling rate of 5°$Cmin^{-1}$ to allow decarbonation and homogenization of the precursors to take place. The mixture was then ball-milled once more for 2 hours in isopropyl alcohol, dried, sieved, and pressed into pellets of green diameter, 20mm or 25mm with a uniaxial pressure of 1MPa; the pellets were then fired in a temperature range of 1150-1500°C with heating/cooling rates of 10°$Cmin^{-1}$.

Samples were initially examined for completeness of reaction and phase-purity by powder XRD with a Siemens D5000 instrument, using Cu Kα radiation. For lattice-parameter determination and Rietveld refinement of the crystal structure, data were collected with the same instrument over the range $15 \le 2\theta \le 120°$ using a stepwidth of 0.03°. Rietveld refinement was performed using the program FullProf [15]. Sample density was determined using the Archimedes method by displacement of water.

Phase composition was analysed with a Jeol Superprobe JXA-8900M electron probe microanalyser; standards were $SrCO_3$ and $CePO_4$; oxygen content was calculated by difference from cation stoichiometries. Microstructure and phase composition were also analysed by SEM with a Zeiss DSM400 instrument.

Stability of $SrCeO_3$ in water was examined in a sealed cell, similar to an autoclave, constructed of a teflon inner casing and steel outer casing (cell volume ≈ 20cm^3). A solid ceramic piece was placed in the cell with 2ml of ultra-pure H_2O and heated over a temperature range of 120-174°C. Under these conditions, the ceramic is exposed to both high pH_2O and superheated water. The water-vapour partial pressure can be approximated using the Clausius-Clapeyron equation:

$$P_2 = P_1 . exp\,[(\Delta_{vap}H_m/R)(1/T_1 - 1/T_2)] \quad (4)$$

where P_1, T_1 and P_2, T_2 are the pressure and temperature of water at the point of vapourisation (1atm., 373K) and test conditions, respectively, $\Delta_{vap}H_m$ is the enthalpy of vapourisation of water and R is the gas constant. The reaction product was determined by powder XRD collected over the range $10 \le 2\theta \le 70°$.

3. RESULTS

3.1 Phase analysis

3.1.1. XRD AND SEM

All compositions formed the orthorhombic $SrCeO_3$ perovskite structure (ICDD no. 47-1689) as the main phase on final firing at 1350°C for 12 hours. For Sr stoichiometric and Sr deficient samples ($x \le 1$), CeO_2 was readily observable during long scans as a second phase in XRD patterns with a peak intensity of I/I_{max} = 5.5% at 2θ= 28.4°, corresponding to the CeO_2 (1 1 1) reflection. X-ray phase-pure material could not be obtained for nominally stoichiometric $SrCeO_3$ or Sr deficient samples for several different processing regimes. Significant amounts of CeO_2 were observed at each stage of several cycles of grinding and refiring in steps of 50°C in the range 1100-1350°C with no observable decrease in intensity of the principal CeO_2 reflections. Degradation of the perovskite took place at 1500°C (Fig. 1). For Sr-excess samples, X-ray phase-pure perovskite was obtained for composition, x = 1.04, on final firing at 1400°C for 12 hours; for 2$mol.\%$ Sr excess, vestiges of CeO_2 were still observed after this time.

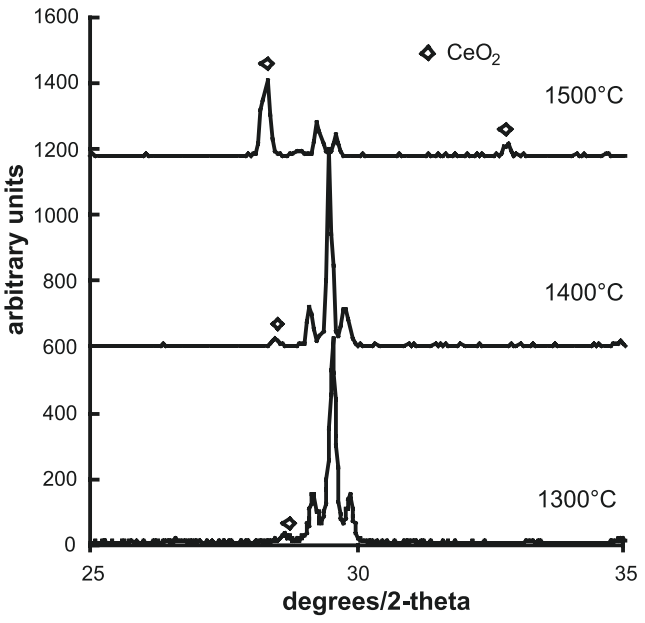

Figure 1. XRD patterns of $SrCeO_3$ sintered at (a) 1300°C, (b) 1400°C and (c) 1500°C.

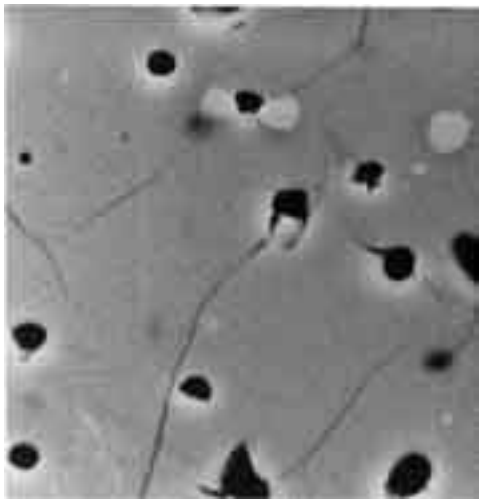

Figure 2. Scanning electron micrograph of nominally stoichiometric $SrCeO_3$ sintered at 1350°C in air showing CeO_2 secondary phase (white).

Fig 2. shows a scanning electron micrograph of nominally stoichiometric $SrCeO_3$ sintered at 1350°C in which CeO_2 appears as the whiter phase; pores are also observed. The densities of samples sintered at 1350°C for 12 hours were higher for the Sr-rich phases: 5.18gcm^{-1}, x = 0.98, 1.0; 5.38gcm^{-1}, x = 1.02; 5.62gcm^{-1}, x = 1.04.

3.1.2 EXPOSURE TO THE ATMOSPHERE

To assess reaction of grain-boundary SrO with the atmosphere, samples of solid pieces were exposed to the laboratory air for several weeks. For both Sr-stoichiometric and Sr–deficient samples, mechanical integrity was obtained during this period. In the case of the Sr–excess sample, x = 1.04, no degradation was observed for ceramics sintered up to 1350°C, but when fired at 1400°C, disintegration of a sintered piece took place over a period of several hours.

Surfaces of the exposed pellets were analysed by SEM, as shown in the scanning electron micrographs, Fig 3, for fractures, (a) x = 0.98, (b) 1.0 and (c) 1.02, and for pellet surface, (d) x = 1.02. No evidence of Sr-related reaction products was detected.

3.1.3 EPMA

The results of EPMA analyses of compositions, x = 0.98, 1.0 and 1.04 fired at 1350°C for 12 hours are shown in Table 1. The composition of the main phases in each case was averaged over 20 spot analyses. Formula were then recalculated normalising for Ce = 1 and estimating oxygen content based on valence states Ce(IV) and Sr(II); in related compositions prepared similarly, the Ce(III) content is very low [16]. For all three samples, Sr excess is observed in accordance with the

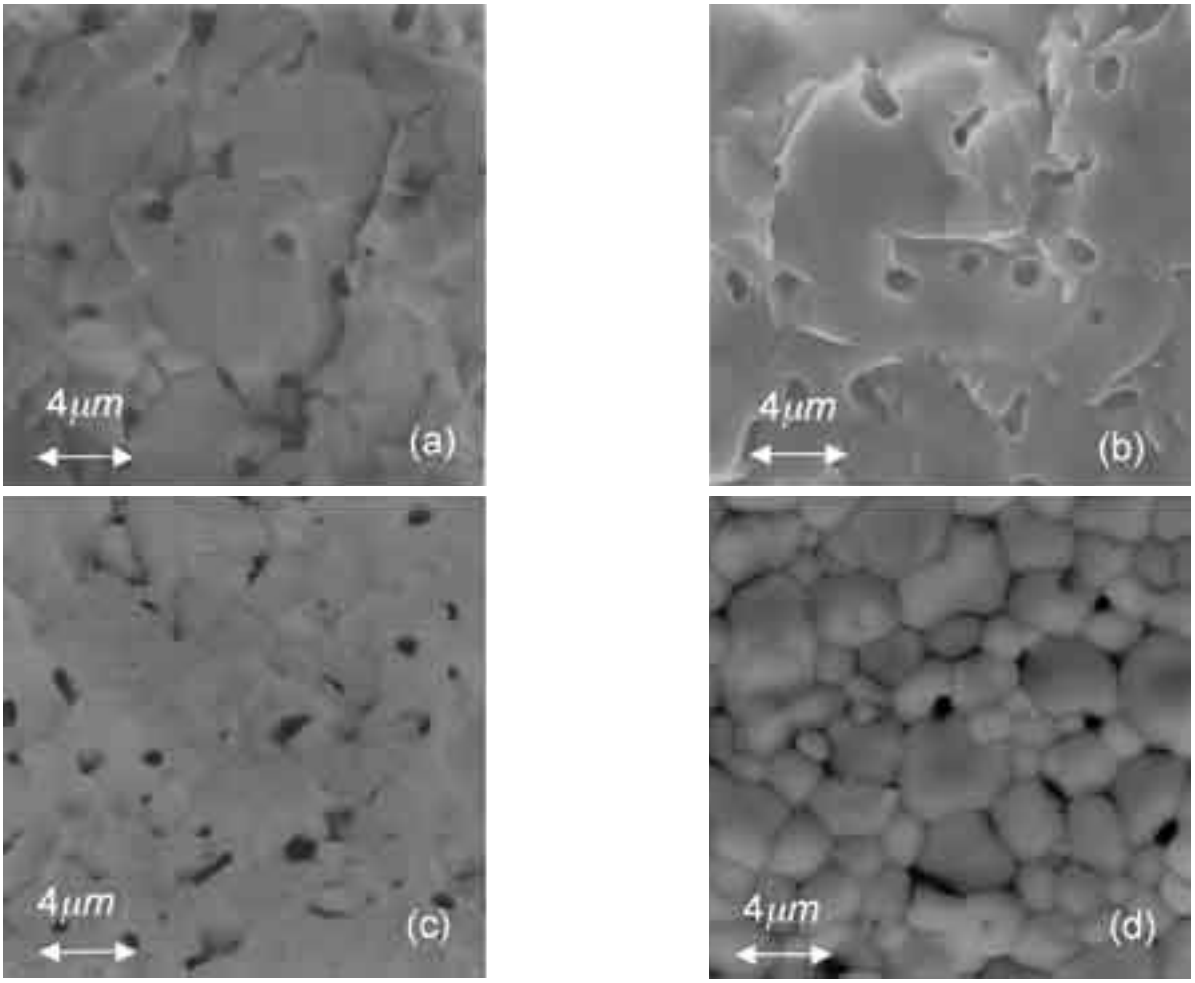

Figure 3. Scanning electron micrographs of $Sr_xCeO_{3\pm\delta}$ fracture surfaces exposed to the air for several weeks: (a) x = 0.98, (b) x = 1.0, (c) x = 1.02; (d) pellet surface of x = 1.02.

TABLE 1. EPMA COMPOSITIONAL ANALYSIS OF $SrCeO_{3+\delta}$

	Starting composition (mol.ratio)		Composition of main phase (mol.ratio)		
Sample	SrO	CeO_2	SrO	CeO_2	Calculated formula[a]
x = 0.98	49.49	50.51	51.1(7)	49.3(4)	$Sr_{1.04}CeO_{3.04}$
x = 1.00	50.0	50.0	50.67(7)	49.60(4)	$Sr_{1.02}CeO_{3.02}$
x = 1.04	50.98	49.02	51.3(2)	49.2(1)	$Sr_{1.04}CeO_{3.04}$

[a]Formula were calculated normalising for a Ce(IV) content of 1.

XRD results. One should note that the contents of x = 0.98 and x = 1.0 fall within the same range (to within e.s.d.'s), whereas the stoichiometry was calculated from the mean contents.

3.2 Structure

Nominally stoichiometric $SrCeO_3$ crystallises with the $GdFeO_3$-type perovskite structure (S.G. Pnma: $a \approx c \approx \sqrt{2}a_p$; $b \approx 2a_p$; $a > c$) as determined from neutron-diffraction data [17,18]*. The structure differs from the more common $GdFeO_3$-type orthorhombic distortion through inversion of the two shorter **a** and **c** axes (Pnma setting).

Refinement was conducted in this study with laboratory-source X-ray data employing the stoichiometric formula, $SrCeO_3$, for all studied compositions starting with the structural parameters for $SrCeO_3$ obtained by Knight and Bonanos [17]. For samples $x \leq 1$, regions of the diffractograms containing CeO_2 reflections were omitted from refinement, whereas for x = 1.04, the entire pattern was modelled. Observed and difference diffraction profiles of $Sr_{1.04}CeO_{3\pm\delta}$ are shown in Fig. 4, with structural and refinement parameters given in Table 2. Unit-cell data and bond-lengths for the three refined samples are given in Tables 3(a) and (b), respectively.

In accordance with the limited compositional variance exhibited among the three studied samples, no significant structural differences were observed. A slightly lower cell volume was found for composition x = 0; analogously, the average Ce-O and Sr-O bond lengths are very slightly lower for x = 0.

Analysis of the occupation and thermal vibration factors for the atomic sites may, in favourable cases, assist in the determination of the defect chemistry. Refinement was also conducted, therefore, with possible Sr-excess compensation mechanisms. However, the results of this analysis were equivocal since the changes in ion occupancies were too small to result in significant improvements in the refinement parameters. Occupancy differences were largely compensated by changes in the thermal vibration factors.

On employing the stoichiometry, $SrCeO_3$, the Sr and O thermal parameters for compositions x = 0.98 and 1.0, were physically sensible whereas the Ce thermal parameter was rather low, close to zero (x = 0.98) or negative (x = 1.0). Ranløv *et. al*. [18] also obtained negative thermal vibration parameters on the Ce site when refining $SrCeO_3$ from neutron-diffraction data whereas the thermal parameters obtained by Knight et al. [17] are physically more reasonable.

The low B-site thermal-vibration parameters *may* preclude certain SrO excess compensation mechanisms from conside-

*Knight et.al. (16) used the Pmcn setting of S.G. No. 62, ($a \approx 2a_p$; $b \approx c \approx \sqrt{2}a_p$; $b < c$).

TABLE 2. CRYSTAL STRUCTURE PARAMETERS FOR $Sr_{1.04}CeO_{3+\Delta}$

Pnma; a = 6.14128(4), b = 8.57116(6), c = 5.99985(4)Å; V = 315.820(4)Å^3

atom	site	x/a	y/b	c/z	B_{iso} (Å^2)	Occupancy (n)
Sr(1)	*4c*	-0.0452(2)	¼	0.0114(5)	0.77(4)	1.0[a]
Ce(1)	*4b*	0	0	½	0.30(2)	1.0
O(1)	*4c*	0.046(2)	¼	0.605(2)	0.7(2)	1.0
O(2)	*8d*	0.301(1)	-0.057(1)	0.698(1)	0.7(2)	1.0

R_p = 9.26, R_{wp} = 12.9, R_B = 3.61, R_F = 3.18, R_{exp} =7.70%

[a] Occupancies are for nominal $SrCeO_3$ stoichiometry

TABLE 3.

(a) UNIT CELL PARAMETERS FOR THE $Sr_xCeO_{3\pm\delta}$ SYSTEM.

Composition (x)	a (Å)	b (Å)	c (Å)	V (Å^3)
0.98	6.14241(6)	8.57373(8)	6.00235(5)	316.104(5)
1.0	6.13117(6)	8.56042(9)	5.99445(6)	314.621(5)
1.04	6.14128(4)	8.57116(6)	5.99985(4)	315.820(4)
1.0[a]	6.14830(16)	8.58330(24)	6.00894(16)	317.11(2)

[a]Unit-cell data for neutron refined $SrCeO_3$ from Ref. [17]; parameters shown for setting Pnma.

(b) METAL-OXYGEN BOND LENGTHS (Å) IN THE $Sr_xCeO_{3\pm\delta}$ SYSTEM

Bond	x = 0.98	x = 1.0	x = 1.04
Ce-O1 × 2	2.255(4)	2.263(4)	2.251(4)
Ce-O2 × 2	2.23(1)	2.22(1)	2.240(6)
Ce-O2 × 2	2.26(1)	2.25(1)	2.251(6)
Sr-O1 × 1	2.49(1)	2.46(1)	2.50(1)
Sr-O1 × 1	2.62(1)	2.61(1)	2.61(1)
Sr-O2 × 2	2.49(1)	2.51(1)	2.498(7)
Sr-O2 × 2	2.87(1)	2.86(1)	2.871(7)
Sr-O2 × 2	3.07(1)	3.06(1)	3.065(8)
Ce-O average	2.25	2.24	2.25
Sr-O average	2.75	2.74	2.75

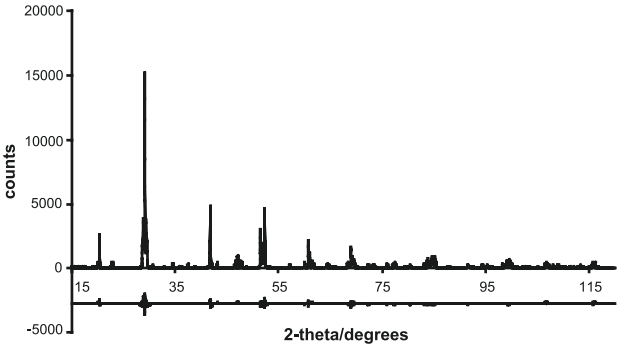

Figure 4. Observed and difference XRD diffraction profiles of $Sr_{1.04}CeO_{3+\delta}$.

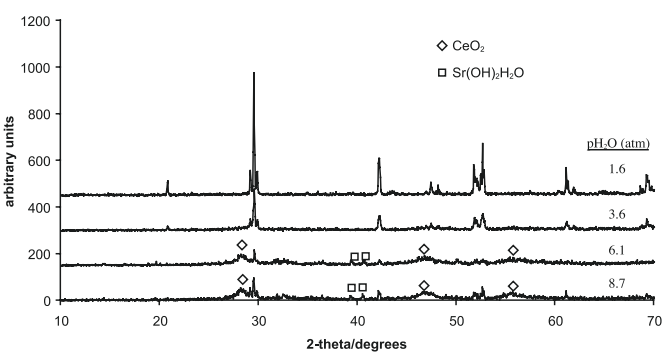

Figure 5. XRD patterns of $SrCeO_3$ after exposure to H_2O showing degradation with increasing pH_2O. Unmarked reflections correspond to perovksite phase.

ration, such as the formation of B-site vacancies, since the refinement model indicates that more electron density on this site is required. However, it is not known at this stage if the low values arise from an incomplete structural model for the Sr-excess samples or experimental anomalies. Thermal vibration parameters may have correlated with the background or absorption phenomena giving rise to distorted values. Equally, some subtle structural complexities may be present which are not detectable with the average structures obtained from neutron or X-ray data. In any case, the structural model does not adequately describe the accommodation of Sr excess. Further work involving electron diffraction and conductivity studies is, therefore, required to permit an interpretation of the accommodation or otherwise of excess SrO, and of the accompanying defect-compensation mechanism.

3.3 Stability of $SrCeO_3$ in H_2O

The stability of $SrCeO_3$ in water was examined by exposing pellet fragments for a period of 2 hours in the reaction vessel within a temperature range of 120-174°C, corresponding to a pH_2O range of 1.6-8.7*atm*. At $pH_2O \approx 1.6atm$, the perovskite phase is stable throughout the exposure period. However, at $pH_2O \approx 3.6atm.$, the sample begins to degrade at the surface, and at higher pH_2O broad reflections of CeO_2 are observed in the XRD pattern together with reflections of $Sr(OH)_2.H_2O$. We can formulate the reaction between water and the perovskite as:

$$SrCeO_3\ (s) + 2H_2O\ (s/g) \rightarrow CeO_2\ (s) + Sr(OH)_2.H_2O\ (s/l) \quad (5)$$

Fuel-cell operating conditions based on a proton-conducting oxide (~ 0.1 *atm.* pH_2O) would be much less severe than those encountered in the reaction cell. However, long-term use in atmospheres with high pH_2O for $SrCeO_3$-based compositions may lead to membrane degradation, especially at the solid-gas interface. Similar results for the instability of $BaCeO_3$ in water have been reported by Tanner and Virkar [19].

4. DISCUSSION

The phase analyses suggest that $SrCeO_3$ displays limited compositional variation with a minimum in free energy occurring for Sr superstoichiometric compositions. In the present study we were unable to obtain nominally stoichiometric $SrCeO_3$, although it is possible that very long sintering times or alternative synthesis methods may produce phase-pure material. Further work is, needed, therefore, to separate the effects of kinetic and thermodynamic factors on the phase formation. It is conceivable that other authors may also not have obtained stoichiometric $SrCeO_3$. For example, in the work of Gopalan and Virkar [20], a shoulder on the main cluster of perovskite peaks appears at 28-29° in the region of the most intense CeO_2 reflection, whereas in the structural determination of $SrCeO_3$ of Ranløv et.al. [18], the region of 2θ corresponding to the most intense CeO_2 peak (2θ = 44.98, for λ = 2.41064Å) was omitted from refinement.

An alternative possibility to bulk accommodation is that the SrO excess is located entirely in the grain boundaries. As mentioned previously, disintegration of sintered bodies may take place in the case of nominally stoichiometric phases, indicating that only very small quantities of grain-boundary SrO are required to affect mechanical breakdown. However, SEM analysis did not indicate the presence of Sr reaction products after long-term exposure to the air, with disintegration only occurring for a sample with 4*mol.%* excess SrO when sintered at 1400°C. It is unlikely, therefore, that the amounts of SrO present in the grain boundaries are high enough to account for the excess of SrO designated by both the nominal stoichiometry (x >1) or phase analysis (all x). The fact that the composition of the main phase is Sr-rich for samples with nominal Sr deficiency is supportive evidence that the high Sr content is not a consequence of incomplete reaction. Nevertheless a more detailed study of the grain boundary should be undertaken by TEM to explore the possibility of a high intergranular SrO content.

The ideal composition may be Sr-rich as a result of the instability of $SrCeO_3$ arising form the mismatch of the Sr and Ce cation radii in the perovskite structure. Yokakawa *et.al.* [21] have shown that an approximate correlation exists between the enthalpy of formation of perovskites from their binary oxides and the Goldschmidt tolerance factor for perovskites ($t = (r_A + r_{O)} / \sqrt{2}(r_B + r_O)$). $SrCeO_3$ has a tolerance factor of 0.886, which is at the lower limit for observed perovskites. The enthalpy of formation of $SrCeO_3$ from SrO and CeO_2 is accordingly very low (~ 4 $kJmol^{-1}$), such that it is unstable with respect to the constituent oxides below ≈ 366°C [20]. Hence, the low phase stability appears to arise from the effects of lattice strain brought about by the considerable deviation from the ideal perovskite structure on accommodating a small A cation (Sr) and large B cation (Ce). This mismatch between A and B cations is possibly alleviated by elimination of some Ce from the stoichiometric composition. It follows from consideration of the tolerance factor that a compensation mechanism involving partial occupation of the B-site with Sr^{2+} (1.16*Å* in VI coordination) for Ce^{4+} (0.87*Å* (VI)) [22] is likely to be highly unfavourable for geometric reasons.

There are some parallels between the behaviour of $SrCeO_3$ and that found for $BaCeO_3$ in the work of Haile and coworkers [8,9]. Whereas BaO deficiency is not tolerated in $BaCeO_3$, BaO excess may be accommodated in the main phase up to 4*mol.%* with accompanying expansion of the unit cell, indicative of BaO excess in the bulk phase. Sinterability also increases for both AO-rich $SrCeO_3$ and $BaCeO_3$, although it is unclear whether this may be due in part to liquid-phase assisted sintering of intergranular AO or improved diffusion kinetics on introducing defects.

5. SUMMARY AND CONCLUSIONS

Phase formation and structural properties of $SrCeO_3$ with cation nonstoichiometry have been investigated for compositions, $Sr_{1\pm x}CeO_{3\pm\delta}$ ($0.98 \le x \le 1.04$). Whereas a number of studies have employed A-site substoichiometry to improve phase stability, $SrCeO_3$ does not accommodate Sr deficiency. In contrast, samples with SrO excess (4*mol.%*) may be readily synthesised by solid-state reaction. Phase analyses by EPMA indicate that little variation from an approximate composition $Sr_{1.04}CeO_{3+\delta}$ is observed for all x. Although preliminary work indicates that the SrO excess is primarily accommodated in the bulk rather than intergranular regions, more detailed analyses of the grain-boundary is required.

The stability of nominally stoichiometric $SrCeO_3$ was examined in an atmosphere of high pH_2O for 2 hours, degrading to $Sr(OH)_2.H_2O$ and CeO_2 at a $pH_2O \geq 3.6atm$.

ACKNOWLEDGEMENTS

One of the authors (GCM) is sponsored by the EU RTN programme High Temperature Proton Conductors (HiTP) "Investigation of high temperature solid proton conductors of relevance to fuel processing and energy conversion applications".

REFERENCES

1. T. Norby, Solid-state protonic conductors: principles, properties, progress and prospects, Solid State Ionics, **125**, 1-11 (1999).
2. N. Bonanos, Transport properties and conduction mechanism in high temperature proton conductors, Solid State Ionics, **53-56**, 967-974 (1992).
3. H. Iwahara, Oxide-ionic and protonic conductors based on perovskite-type oxides and their possible applications, Solid State Ionics, **52**, 99-104 (1992).
4. J. Guan, S.E. Dorris, U. Balachandran, M. Lin, Transport properties of $SrCe_{0.95}Y_{0.05}O_{3-\delta}$ and its application for hydrogen separation, Solid State Ionics, **110**, 303-310 (1998).
5. N. Bonanos, B. Ellis, K.S. Knight and M.N. Mamood, Ionic Conductivity of Gadolinium-doped Barium Cerate Perovskites, Solid State Ionics, **35**, 179-188 (1989).
6. R.A. Davies, M.S. Islam, J.D. Gale, Dopant and proton incorporation in perovskite-type zirconates, Solid State Ionics, **126**, 323-335 (1999).
7. D. Yang, A.S. Nowick, J. Am. Ceram. Soc., **78**, 3033-3039 (1995).
8. D. Shima and S.M. Haile, The influence of cation nonstoichiometry on the properties of undoped and gadolinia-doped barium cerate, **97**, 443-455, (1997).
9. S.M. Haile, G. Staneff, K.H Ryu, Non-stoichiometry, grain boundary transport and chemical stability of proton conducting perovskites, J. Mat. Sci., **36**, 1149-1160 (2001).
10. G. Ma, H. Matsumoto, H. Iwahara, Ionic conduction and nonstoichiometry in non-doped $Ba_xCeO_{3-\alpha}$, Solid State Ionics, **122**, 237-247 (1999).
11. K.D. Kreur, E. Schönherr, J. Maier, in Proceedings of the 14th Risø International Symposium on Materials Science, Risø Natl. Lab., Roskilde, Denmark 1993.
12. D.P. Fagg, V.V. Kharton, A.V. Kovalesky, A.P. Viskup, E.N. Naumovich, J.R. Frade, The stability and mixed conductivity in La and Fe doped $SrTiO_3$ in the search for potential SOFC anode materials, J. Eur. Ceram. Soc., **21**, 1831-1835 (2001).
13. A.A. Ferreira, J.A. Labrincha, J.R. Frade, Transport properties of Sr_{1-x}(Zr, Y, Ti)O_3 compositions with improved sinterability, Solid State Ionics, **77**, 210-214 (1995).
14. V.V. Kharton, A.V. Kovalevsky, E.V. Tsipis, A.V. Viskup, E.N. Naumovich, J.R. Jurado, J.R. Frade, Mixed conductivity and stability of A-site-deficient $Sr(Fe,Ti)O_{3-\delta}$ perovskites, J. Solid State Electrochem., **7**, 30-36 (2002).
15. FullProf, J. Rodriguez-Carvajal, in "Satellite Meeting on Powder Diffraction", Abstracts of the XVth Conference on the Internation Union of Crystallography, Toulouse, 1990, 127.
16. A. Kruth, J.T.S. Irvine, Water incorporation studies on doped barium cerate perovskites, Solid State Ionics,168-163, 83-91 (2003).
17. K.S. Knight and N. Bonanos, The crystal structures of some doped and undoped alkaline earth cerate perovskites, Mat. Res. Bull., **30**, 347-356 (1995).
18. J. Ranløv, B. Lebech and K. Nielsen, Neutron diffraction investigation of the atomic defect structure of Y-doped $SrCeO_3$, a high-temperature protonic conductor, J. Mater. Chem., **5**, 743-747 (1995).
19. C.W. Tanner, and A.V. Virkar, Instability of $BaCeO_3$ in H_2O-containing Atmospheres, J. Electrochem. Soc., **142**, 1386-1389 (1996).
20. S. Gopalan and A.V. Virkar, Thermodynamic Stabilities of $SrCeO_3$ and $BaCeO_3$ Using a Molten Salt Method and Galvanic Cells, J. Electrochem. Soc., **140**, 1060-1065 (1993).
21. H. Yokokawa, T. Kawada, M. Dokiya, Thermodynamic regularities in perovskite and K_2NiF_4 compounds, J. Am. Ceram. Soc., **72**, 152-153 (1989).
22. Revised Effective Ionic Radii and Systematic Studied of Interatomic Distances in Halides and Chalcogenides, R.D. Shannon, Acta. Cryst., **A32**, 751-767, (1976).

Recibido: 13.12.02
Aceptado: 24.08.03

Fallece Don José Lahuerta

Desde la Sociedad Española de Cerámica y Vidrio queremos expresar nuestra condolencia a los familiares y colaboradores de **D. José Lahuerta** recientemente fallecido. A lo largo de su vida profesional demostró junto con su familia y empresa un continuo apoyo a la vida asociativa del sector. En particular, como veterano miembro de la SECV, siempre encontramos su ayuda en las actividades que celebramos en su región. Su fallecimiento se ha producido justamente cuando trabajaba como miembro del Comité Organizador del XLIII Congreso de la SECV que celebraremos del 19 al 22 de Noviembre en Manises. Ha muerto pues, como vivió, contribuyendo al desarrollo de su mundo y el nuestro, la cerámica. En Manises, durante el Congreso le ofrceremos el homenaje público que se merece.